1521-0103/358/2/282–293$25.00
THE JOURNAL OF PHARMACOLOGY AND EXPERIMENTAL THERAPEUTICS

http://dx.doi.org/10.1124/jpet.116.233908
J Pharmacol Exp Ther 358:282–293, August 2016

Autophagy Inhibition Delays Early but Not Late-Stage Metastatic Disease[S]

Rebecca A. Barnard, Daniel P. Regan, Ryan J. Hansen, Paola Maycotte, Andrew Thorburn, and Daniel L. Gustafson

Department of Clinical Sciences, Colorado State University, Fort Collins, Colorado (R.A.B., D.P.R., R.J.H., D.L.G.); and Department of Pharmacology, University of Colorado School of Medicine, Aurora, Colorado (P.M., A.T.)

Received March 24, 2016; accepted May 23, 2016

ABSTRACT

The autophagy pathway has been recognized as a mechanism of survival and therapy resistance in cancer, yet the extent of autophagy's function in metastatic progression is still unclear. Therefore, we used murine models of metastatic cancer to investigate the effect of autophagy modulation on metastasis development. Pharmacologic and genetic autophagy inhibition were able to impede cell proliferation in culture, but did not impact the development of experimentally induced 4T1 and B16-F10 metastases. Similarly, autophagy inhibition by adjuvant chloroquine (CQ) treatment did not delay metastasis in an orthotopic 4T1, tumor-resection model. However, neoadjuvant CQ treatment or genetic autophagy inhibition resulted in delayed metastasis development, whereas stimulation of autophagy by trehalose hastened development. Cisplatin was also administered either as a single agent or in combination with CQ. The combination of cisplatin and CQ was antagonistic. The effects of autophagy modulation on metastasis did not appear to be due to alterations in the intrinsic metastatic capability of the cells, as modulating autophagy had no impact on migration, invasion, or anchorage-independent growth in vitro. To explore the possibility of autophagy's influence on the metastatic microenvironment, bone marrow–derived cells (BMDCs), which mediate the establishment of the premetastatic niche, were measured in the lung and in circulation. Trehalose-treated mice had significantly more BMDCs than either vehicle- or CQ-treated mice. Autophagy inhibition may be most useful as a treatment to impede early metastatic development. However, modulating autophagy may also alter the efficacy of platinum-based therapies, requiring caution when considering combination therapies.

Introduction

Macroautophagy (hereafter called autophagy) is a lysosomal degradation process characterized by self-consumption of cytoplasmic material. One of the defining features of this process is the formation of distinctive double-membraned vesicles, called autophagosomes, used to traffic cargo intended for degradation (Mizushima et al., 2010). Although initially identified as a starvation response, autophagy is involved in the overall maintenance of the cell, including the potential for cancer development. Autophagy's role in cancer is complex. Autophagy may be tumor-suppressive, as it acts as a cellular quality-control mechanism. Mice deficient in autophagy show accumulation of aberrant organelles and misfolded proteins, potentially leading to elevated levels of reactive oxygen species, inflammation, and genomic instability (Ichimura and Komatsu, 2011). However, established tumors may also use autophagy as a cytoprotective mechanism to remove toxic oxygen radicals or damaged proteins that can trigger apoptosis (Gewirtz, 2014). Elevated levels of autophagy have been observed in many tumor types and are correlated with a more metastatic and aggressive phenotype. Inhibiting autophagy in vitro can increase tumor cell death and sensitize cells to some chemotherapy (Lazova et al., 2012). Taken together, autophagy appears to act as a mechanism of chemoresistance or survival in tumor cells and has prompted the clinical investigation of autophagy inhibition as a means to sensitize cells to chemotherapy or radiation (Barnard et al., 2014; Mahalingam et al., 2014; Rangwala et al., 2014a,b; Rosenfeld et al., 2014; Vogl et al., 2014).

Metastasis remains the major cause of death from cancer, and although a number of studies have begun to explore the role of autophagy in metastasis, it is still unclear whether autophagy is pro- or antimetastatic (Kenific et al., 2010). One of the first steps in the metastatic cascade is the ability of cells to invade and escape the primary tumor. One study demonstrated that activation of the autophagy complex ULK-1/Fip200

This work was supported by the National Institutes of Health National Cancer Institute [Grant 1R01CA150925 Role of Autophagy in Tumor Cell Death] and the University of Colorado Cancer Center Support [Grant P30CA046934] for work conducted in the Pharmacology Shared Resource.
dx.doi.org/10.1124/jpet.116.233908.
[S] This article has supplemental material available at jpet.aspetjournals.org.

ABBREVIATIONS: AUC, area under the curve; Baf A1, bafilomycin A1; BMDC, bone marrow–derived cell; CQ, cholorquine; Ct, cycle threshold; DMEM, Dulbecco's modified Eagle's medium; FBS, fetal bovine serum; PBS, phosphate-buffered saline; RT, room temperature; RT-qPCR, reverse-transcription quantitative polymerase chain reaction; shRNA, short hairpin RNA; Tbp, TATA binding protein; VEGFR, vascular endothelial growth factor receptor; VLA-4, Integrin $\alpha4\beta1$ very late antigen-4.

was instrumental in inhibiting cell motility. Cells were more invasive when autophagy was inhibited, particularly under metabolic stress (Caino et al., 2013). In addition, autophagy has been shown to be integral in β1-integrin receptor internalization and degradation (Tuloup-Minguez et al., 2013). Autophagy can also suppress tumor necrosis and macrophage infiltration, which is required for invasion and metastasis in some tumor types, such as the PyMT model of breast cancer (Degenhardt et al., 2006; DeNardo et al., 2009). Yet other studies reported that autophagy inhibition reduced invasion in three-dimensional organotypic models of glioma and RAS-driven invasion (Macintosh et al., 2012; Lock et al., 2014). Once cells have detached from the extracellular matrix, autophagy may be crucial for survival (Avivar-Valderas et al., 2011). Normally, cells undergo apoptosis if they detach from the extracellular matrix, also known as anoikis, due to increased metabolic and oxidative stress (Kenific et al., 2010). Autophagy is induced in detached breast cancer epithelial cells and is necessary for their continued survival (Fung et al., 2008). In a model of hepatocellular carcinoma, autophagy inhibition did not alter invasion or migration, but could attenuate anchorage-independent growth (Peng et al., 2013). Additionally, autophagy levels appeared highest in early metastatic lesions, and autophagy was only necessary in the lung-colonization stage. Autophagy could allow for resistance to anoikis and facilitate colonization. As in primary tumor development, more study is still needed to understand autophagy's apparent contradictory role in metastasis and to reconcile seemingly conflicting results.

Adding another layer to the complexity is autophagy's immunomodulatory functions and the use of immune-deficient mouse models (Bristol et al., 2013). The functionality of the immune system can influence the efficacy of combining autophagy inhibition with anticancer therapies (Michaud et al., 2011). Therefore, it is important to consider the effect of autophagy in an immune-competent model. Since it is still unclear what role autophagy plays in metastatic progression, and few models have examined autophagy in an immune-competent model, we investigated the effect of autophagy modulation on multiple steps in the metastatic cascade utilizing multiple cancer models both in vitro and in vivo. Additionally, we examined autophagy modulation in clinically relevant surgical adjuvant and neoadjuvant syngeneic mouse models.

Materials and Methods

Cell Lines and Cell Culture. The 4T1-luc and B16-F10 cell lines were generously provided by Dr. S. Dow at Colorado State University (Fort Collins, CO). The DLM8 line was provided by Dr. D. Thamm at Colorado State University. Cells were validated as murine in origin in April 2012 and used within 6 months of thawing. All cell lines were maintained in Dulbecco's modified Eagle's medium (DMEM; Cellgro, Manassas,VA) with 10% fetal bovine serum (FBS; Cellgro), 5% penicillin+streptomycin (Hyclone Laboratories Inc., Logan, UT), and 1 mM sodium pyruvate (Cellgro) at 37°C and 5% CO_2.

Becn 1 and Atg7 Knockdown. Lentiviral particles containing a pKLO vector with Becn 1 (TRCN0000087288) or Atg7 (TRCN0000092167) mouse short hairpin RNA (shRNA) were made in HEK293FT cells. 4T1-luc, B16-F10, and DLM8 cells were transduced with the lentiviruses containing the pKLO Becn 1 shRNA, Atg7, or a nonsilencing shRNA using 8 μg/ml polybrene (Sigma-Aldrich, St. Louis, MO). Puromycin (2 μg ml; Calbiochem, San Diego, CA) was used for 1 week to select for successfully transduced cells. Becn 1 or Atg7 knockdown was confirmed by western blot and reverse-transcription quantitative polymerase chain reaction (RT-qPCR).

Serum Starvation Assay. To confirm successful inhibition of autophagy due to Becn1 or Atg7 knockdown, cells were treated with Earl's Balanced Salt Solution (Hyclone Laboratories) with or without 10 μM cholorquine (CQ; Sigma-Aldrich) or 5 nM bafilomycin A1 (Baf A1; Sigma-Aldrich) for 2 hours. Protein was then isolated, and LC3 processing was measured by western blot.

Western Blot Analysis. After treatment, cells or tissues were lysed with a lysis buffer [0.01% Triton X-100, 150 mM NaCl, 10 mM Tris (pH 7.5), 0.2 mM Na-orthovanadate, 34.8 μg/ml phenylmethylsulfonyl fluoride, and 1× Protease Inhibitor Cocktail (Roche, Basel, Switzerland)]. Following electrophoresis and transfer, blots were blocked in 2.5% milk and probed with anti-LC3 antibodies (Novus Biologicals, Littleton, CO) at 1:1000, anti–beclin-1 antibodies (Novus Biologicals) at 1:2000, anti-Atg7 antibodies (Novus Biologicals) at 1:500, anti-actin antibodies (Sigma-Aldrich) at 1:5000, or anti-tubulin antibodies (Sigma-Aldrich) at 1:5000. After overnight incubation at 4°C, anti-rabbit (Thermo Scientific Pierce, Waltham, MA) or anti-mouse (Thermo Scientific Pierce) secondary antibodies conjugated to horseradish peroxidase were applied. Blots were developed using West Dura (Thermo Scientific Pierce) and imaged in a ChemiDoc XRS^+ (Bio-Rad, Hercules, CA) using Image Laboratories version 3.0 software (Bio-Rad) for analysis. Densitometry was measured using ImageJ64 (National Institutes of Health, Bethesda, MD), and target protein was normalized to actin or tubulin.

RT-qPCR Analysis. To quantitate Becn 1 or Atg7 knockdown, qPCR was used to compare mRNA expression. RNA was isolated using the RNeasy kit (Qiagen, Hilden, Germany) per the manufacturer's instructions with on-column DNase I digestion (Qiagen). The concentration and purity of the RNA was measured using a Nanodrop 1000 (Thermo Scientific, Waltham, MA) with ND-1000 version 3.8.1 software. One microgram of RNA was used to synthesize cDNA using a QuantiTect kit (Qiagen) following the included protocol. The reaction took place in an MJ Mini Personal Thermal Cycler (Bio-Rad). A single cycle of 30 minutes at 42°C and 3 minutes at 95°C was used. Negative controls containing no reverse transcriptase were run simultaneously. Primers were designed using Primer-BLAST (National Center for Biotechnology Information, Bethesda, MD). The forward primer for Becn 1 was CCAGCCTCTGAAACTGGACA, and the reverse primer was GCCTGGGCTCTGGTAACTAA. The forward primer for Atg7 was ATGCCAGGACACCCTGTGAA, and the reverse primer was AAGGTATCAAACCCCAAGGCA. Hsp90ab1 (Hsp90) and TATA binding protein (Tbp) were not significantly changed across all cell types and were used as reference genes. The forward primer for Hsp90 was CCCACCACCCTGCTCTGTACTACT, and the reverse primer was GCCTGAAAGGCAAAGGTCTCCACC. The forward primer for Tbp was GGACCAGAACAACAGCCTTC, and the reverse primer was CCGTAAGGCATCATTGGACT. A concentration of 100 nm for the forward primer and 300 nm was used in the reaction. Master mix containing SYBR Green dye was used (iQ SYBR Green Supermix; Bio-Rad). A total reaction volume of 25 μl and 100 ng of cDNA was used. Amplification was measured by fluorescence using the Mx3000p and analyzed using the Mx3000p version 2.0 software (Stratagene, San Diego, CA). One cycle of 95°C for 10 minutes followed by 40 cycles of 95°C for 30 seconds and 60°C for 1 minute were used. A dissociation curve cycle was also added to confirm that a single product was being amplified. Amplification efficiencies were determined using a standard curve of serially diluted cDNA samples with an efficiency of 97.8% for Becn 1, 92.4% for Atg7, 92.7% for Tbp, and 103.2% for Hsp90. All samples were run in triplicate. Samples were compared by subtracting the geometric mean of Ct (cycle threshold) values for Hsp90 and Tbp from Becn 1 and Atg7 to give the ΔCt. The ΔCt was then transformed into $2^{(-\Delta Ct)}$ (Pfaffl, 2001).

Proliferation Assays. Cells were seeded into 96-well tissue culture plates. For anchorage independent growth assays, plates were coated with PolyHEMA (Sigma-Aldrich). Cells were allowed to attach for 24 hours (adherent) or immediately dosed with 10 μM CQ, 5 nM

Baf A1, 100 mM trehalose (Alfa Aesar, Haverhill, MA), cisplatin (Pfizer, New York, NY) IC_{50}, or vehicle for 72 hours. Cisplatin IC_{50} was determined as described in the Supplemental Methods. Knockdown or nonsilencing control lines were grown for 72 hours. Metabolically active cells were visualized with 10% Alamar Blue [200 μg/ml resazurin salt in phosphate-buffered saline (PBS); Sigma-Aldrich] and incubated for 2 hours. Plates were read at 530/590 nm excitation/emission in a Synergy HT plate reader (BioTEK, Winooski, VT). All experiments were repeated in triplicate.

Invasion and Migration Assays. Invasion and migration assays (BD Biosciences, San Jose, CA) were performed according to the manufacturer's instructions. In brief, cells were seeded at 12,500 per well in serum-free DMEM media with 10 μM CQ, 5 nM Baf A1, 100 mM trehalose, or vehicle in triplicate. DMEM with 10% FBS was used as a chemoattractant. Cells were incubated for 20 hours and then stained with 4 μg/ml Calcein dye (Invitrogen, Carlsbad, CA) for 1 hour. Plates were read at 494/517 nm excitation/emission in a Synergy HT plate reader.

Animals. All animal studies were performed in accordance with Colorado State University's Animal Care and Use Committee. 6- to 8-week-old female Balb/c and C57Bl/6J mice were purchased from the National Cancer Institute (Bethesda, MD) or The Jackson Laboratory (Bar Harbor, ME). For experimental metastasis studies, mice were pretreated for 72 hours with either 60 mg/kg chloroquine diphosphate salt (Sigma-Aldrich) or 0.9% saline given by i.p. injection. This dosing regimen was demonstrated to be effective in Maycotte et al. (2014). Mice continued to receive CQ or vehicle daily until the end of the study. Three hundred thousand 4T1-luc or B16-F10 cells in serum-free DMEM media were injected into the tail vein of Balb/c or C57Bl/6J mice. Additional Balb/c mice, not receiving CQ, were challenged with either 4T1-luc cells pretreated with 10 μM CQ for 2 hours or 4T1-luc Becn 1 knockdown cells. For detection of 4T1 luciferase-positive metastases, mice were injected with 50 μl of 30 mg/ml luciferin (Gold Biotechnology, St. Louis, MO) i.p. 5 minutes before being anesthetized with isoflurane. Mice were imaged thrice weekly using the IVIS-100 Imaging System (PerkinElmer, Waltham, MA) with a 1-minute exposure and medium sensitivity setting. Once metastases were visible within the lung, mice were sacrificed. Mice challenged with B16-F10 cells were weighed daily and sacrificed after 10% weight loss.

For surgical adjuvant studies, 1×10^6 4T1-luc cells in 100 μl of serum-free DMEM were implanted subcutaneously into the fourth mammary fat pad of Balb/c mice. Tumor volume was measured with digital calipers using the formula short diameter^2 $\times$ long diameter $\times$ 0.5. Once tumors reached 100 mm^3, they were removed, and mice began treatment 24 hours after, receiving either 60 mg/kg CQ (i.p. daily), a human equivalent exposure of cisplatin at 3 mg/kg (i.p. once every 14 days), a combination of both, or vehicle. Mice were imaged thrice weekly until the appearance of luciferase-positive metastases in the lungs.

For neoadjuvant studies, 4T1-luc, 4T1-luc Becn 1 knockdown, or 4T1-luc nonsilencing cells were implanted in Balb/c mice, and treatment began 24 hours after, similar to the surgical adjuvant studies. For autophagy stimulation, 2% trehalose or 2% sucrose was dissolved in drinking water and given ab libitum. After tumors reached 100 mm^3, they were removed, and mice were imaged thrice weekly until luciferase-positive metastases were visible in the lungs, for survival studies, or 15 days after starting treatment.

Determination of a Human Equivalent Exposure of Cisplatin in Mice. In one human study comparing the pharmacokinetics of 60 mg/m^2 cisplatin administered i.v. versus i.p., the 24-hour plasma-free platinum area under the curve (AUC) levels were 8.0 μg*h/ml and 1600 μmol*min/ml, respectively (Casper et al., 1983). In mice, one study demonstrated that a 27-mg/m^2 (9-mg/kg) i.p. dose of cisplatin resulted in plasma total cisplatin AUC of 3228 μg*min/ml (10,758 μmol*min/ml), and another showed that an 18-mg/m^2 (6-mg/kg) dose produced an AUC of 134 μg*min/ml free cisplatin (Kubota et al., 1993; Lopez-Flores et al., 2005). A clinically relevant level of free cisplatin in plasma of mice is considered to be 81–519 μg*min/ml (Reece et al., 1987; van Hennik et al., 1987). Taking into account that the half-life is twice as long in mice compared with humans, and the LD_{10} in nude mice was found to be 3.5 mg/kg weekly, we chose the dose of 3 mg/kg every 14 days (Reece et al., 1987; Taetle et al., 1987; van Hennik et al., 1987).

Flow Cytometry. Upon study completion, whole blood and lungs were collected from mice. Peripheral blood mononuclear cells were isolated by lysing erythrocytes using ACK buffer solution (150 mM NH_4Cl, 10 mM $KHCO_3$, and 0.1 mM Na_2EDTA). Right lung lobes were minced and digested in 2$\times$ collagenase D (Roche) diluted in Hanks' balanced salt solution + 0.1% FBS/EDTA for 30 minutes at 37°C. Following digestion, tissues were triturated using an 18-g needle and filtered through 70-μm cell strainers ($\times$2) (BD Biosciences). Last, red blood cells were lysed using ACK buffer solution, and remaining cells were resuspended in fluorescence-activated cell sorting (FACS) buffer (PBS with 2% fetal bovine serum and 0.05% sodium azide) for immunostaining.

To minimize nonspecific binding, normal mouse serum (Jackson ImmunoResearch, West Grove, PA) and unlabeled anti-mouse CD16/32 (eBiosciences, San Diego, CA) were applied to cells before immunostaining. Cells were then incubated with the following directly labeled rat monoclonal antibodies for 25 minutes at room temperature (RT): mouse VEGFR1 (clone 141522; R&D Systems, Minneapolis, MN) and mouse VLA-4 (clone R1-2; eBiosciences). Cells were washed in FACS buffer (PBS + 2% FBS and 1% sodium azide) and incubated with streptavidin conjugates when necessary. Flow cytometry was conducted using a Dako/CyanADP flow cytometer (Glostrop, Denmark) with Summit software (Beckman Coulter, Brea, CA). Analysis was done with FlowJo software (Ashland, OR).

Immunofluorescence. Left lung lobes were immersion fixed in a 1% paraformaldehyde–lysine–sodium periodate solution (0.2 M lysine-HCL, 0.21 % Na-periodate, pH 7.4) and cryosectioned at 5 μm for immunostaining. Nonspecific binding was blocked by preincubation of sections with either 5% donkey or goat serum (Jackson ImmunoResearch) in 1% bovine serum albumin for 30 minutes at RT. Primary antibody labeling [1:100 anti-LC3 (Novus Biologicals), 1:30 anti-VEGFR1 clone 141522 (R&D Systems), and 1:200 anti–VLA-4 (Abcam, Cambridge, UK)] was performed at RT for 1 hour in 1% bovine serum albumin. After removal of the primary antibody, tissues were washed with PBS-t, followed by addition of the following secondary antibodies (diluted 1:200 in PBST) for 30 minutes at RT: Cy3-conjugated goat anti-rabbit IgG (LC3), Alexa Fluor 647–conjugated donkey anti-rabbit IgG (VLA-4), and Cy3-conjugated donkey anti-rat IgG (VEGFR1) (Jackson ImmunoResearch). Last, tissues were counterstained with DAPI dye, cover slipped, and visualized using an IX83 confocal microscope (Olympus Tokyo, Japan) and a digital camera (Hamamatsu, Hamamatsu City, Japan). Figures were assembled using Photoshop (CS5; Adobe, San Jose, CA).

Multiplex Serum Cytokine Analysis. Serum cytokine analysis was performed on mice in the 4T1 neoadjuvant metastasis studies described previously. Blood was collected via terminal cardiac puncture, and was obtained during the same postsurgical, premetastatic window of this model as the flow cytometric analyses of bone marrow–derived cells (BMDCs) within the lung and blood. Blood was collected into BD microtainer serum separator tubes (Becton, Dickinson and Company, Franklin Lakes, NJ), centrifuged for 5 minutes at 7000 $\times$ g, and serum removed and frozen at -80°C until analysis. Multiplex cytokine analysis was performed using the Novex (Life Technologies) mouse cytokine magnetic 20-plex panel (Thermo Fisher) according to the manufacturer's protocol. In brief, serum samples were diluted 1:2 into assay diluent, and a 7-point standard curve using 1:3 serial dilutions was prepared. Appropriately diluted sample or standard was then added to a 96-well flat-bottom plate, precoated with magnetic antibody beads, and incubated for 2 hours in the dark on an orbital shaker. Following washing, analytes were detected using a biotinylated antibody followed by streptavidin-R-Phycoerythrin (RPE). Samples were analyzed using the Luminex 200 plate reader and XY platform (Austin, TX). The data were then

exported to Excel (Microsoft, Redmond, WA), and analyte concentrations were determined following generation of the standard curve.

Statistics. All statistical analyses were performed in Prism version 5.0a (GraphPad Software, La Jolla, CA). Percent inhibition was determined by dividing the corrected relative fluorescence of the treated or knockdown cells over the corrected relative fluorescence of the controls. Significance of percent inhibition was determined by one-sample *t* test using 0% as a theoretical mean. For time to metastasis in the lung, a log rank and Gehan-Breslow-Wilcoxon analysis was used to compare survival curves. A one-tailed student's *t* test, assuming LC3 II increases after CQ treatment and Becn 1 decreases after shRNA knockdown, was used to compare mean relative density of LC3 II or Becn 1 in mouse tumor samples analyzed by western blot. Student's *t* test was also used to compare mean percentage of cells expressing the specified surface marker in different treatment groups as determined by flow cytometric analysis. A one-way analysis of variance with Bonferroni post-test was used for mean comparison of drug treatment and culture type. For invasion and migration assays, the mean relative fluorescence of the negative control was subtracted from the relative fluorescence of each replicate. A one-way analysis of variance with Bonferroni post-test was used for mean comparison of treatment. A P value of less than 0.05 was considered significant. All error bars represent the standard deviation.

Results

Pharmacologic and Genetic Inhibition of Autophagy. Autophagy was inhibited pharmacologically using chloroquine diphosphate and Baf A1. Although CQ is one of the most commonly used means of inhibiting autophagy, it has non-autophagic effects, and observed sensitivity to CQ could be independent of autophagy (Maycotte et al., 2012). Thus, we chose a second pharmacologic inhibitor of autophagy, Baf A1, which is another lysomotropic agent that blocks autophagy similarly to CQ but does so through a different molecular target (Yoshimori et al., 1991). The mammalian homolog of Atg8, LC3, can be used as a marker for autophagy. LC3 is cleaved and conjugated to phosphatidylethanolamine, termed LC3 II, upon autophagy induction. In addition, it is incorporated onto the surface of autophagosomes, and correlates to the number of autophagosomes present. Therefore, increases in LC3 II are indicative of increased autophagy levels (Mizushima and Yoshimori, 2007). However, LC3 II is degraded in the lysosome as well, so to accurately measure autophagic flux and prevent LC3 II degradation, CQ or Baf A1 was also included in the assay. Doses of 10 μM CQ and 5 nM Baf A1 were sufficient to inhibit autophagy in 4T1 (mammary carcinoma), B16-F10 (melanoma), and DLM8 (osteosarcoma) murine cell lines and have worked previously in other cell lines (Fig. 1A) (Ni et al., 2011; Maycotte et al., 2012). Higher doses of both drugs can be used to achieve more complete inhibition of autophagy, yet these saturating doses approach the IC_{50} (Supplemental Figs. 1 and 2), and the autophagy-independent effects of the drugs may obfuscate the autophagy-dependent effects. Genetic knockdown of autophagy, targeting Becn 1/Atg6 and Atg7, was also performed. By using multiple means of blocking autophagy, any observed effects can more likely be attributed to autophagy inhibition. To create the Becn 1 and Atg7 knockdown cells, a Becn 1, Atg7, or non-silencing shRNA was delivered by lentivirus. After lentiviral transduction, Becn 1 or Atg7 was significantly reduced as determined by western blot and RT-qPCR analysis (Fig. 1, B–D).

To ensure autophagy was successfully inhibited after shRNA knockdown, cells were serum starved for 2 hours, a positive control for autophagy induction (Mizushima and Yoshimori, 2007). When cells were grown in serum-free media, LC3 processing was decreased in the Becn 1 and Atg7 knockdowns compared with the nonsilencing controls (Supplemental Fig. 1).

Autophagy Inhibition Slows Growth In Vitro but Not in Experimentally Induced Metastases. We tested the effect of autophagy inhibition using the aforementioned methods on the proliferation of 4T1, B16-F10, and DLM8 cells. These cell types were selected because they represent different types of cancer, can be used in syngeneic mouse models, and are highly metastatic (Fidler, 1975; Aslakson and Miller, 1992; Asai et al., 1998). In all cell types, all methods of autophagy inhibition were able to significantly reduce proliferation, although CQ only modestly so in B16-F10 cells (P = 0.049) (Fig. 2A). Next, we tested whether similar results could be recapitulated in experimental metastases. As CQ is currently being investigated in clinical trials, has shown efficacy in other preclinical studies, and is considered to have relatively low toxicity, it was used as the pharmacologic autophagy inhibitor for subsequent in vivo experiments (Amaravadi et al., 2011; Barnard et al., 2014; Mahalingam et al., 2014; Rangwala et al., 2014a,b; Rosenfeld et al., 2014; Vogl et al., 2014). Balb/c or C57Bl/6J mice were first pretreated with 60 mg/kg CQ daily for 72 hours, so autophagy would already be inhibited systemically, then challenged with 4T1-luc or B16-F10 cells delivered via the tail vein. Mice continued to receive daily treatment until development of luciferase-positive 4T1 metastases in the lung or 10% weight loss in the B16-F10–challenged mice. To ensure CQ was effectively inhibiting autophagy, expression of LC3 II was measured in the liver, which responds to both CQ and autophagy modulating effects (Ni et al., 2011). LC3 II was increased in CQ-treated mice, indicating pharmacodynamic efficacy (Fig. 2B). In addition, LC3-positive punctae were more readily visible in the tumor-burdened lungs of mice treated with CQ as compared with the more diffuse, cytosolic staining in vehicle-treated mice, indicating accumulation of blocked autophagosomes (Fig. 2C). CQ was not able to delay the development of 4T1 metastases in the lung, nor significantly prolong survival in the B16-F10–challenged mice (Fig. 2, D and E).

To determine if tumor cells with impaired autophagy, rather than the systemic inhibition, would have an altered ability to colonize the lung, Balb/c mice were also challenged with 4T1-luc Becn 1 knockdown cells or 4T1-luc cells that had been treated with 10 μM CQ 2 hours prior to injection. Again, neither Becn 1 knockdown nor CQ pretreatment of the cells delayed metastasis (Fig. 2F).

Autophagy Inhibition Has an Additive Effect in Combination with Cisplatin In Vitro, but Is Antagonistic in a Neoadjuvant Setting. In recent and ongoing clinical trials, autophagy inhibition is explored as a means of chemosensitization or prevention of therapeutic resistance (Amaravadi et al., 2011; Barnard et al., 2014; Mahalingam et al., 2014; Rangwala et al., 2014a,b; Rosenfeld et al., 2014; Vogl et al., 2014). Therefore, we tested the combination of autophagy inhibition and cisplatin, a clinically relevant therapeutic for all three cancer types being investigated here (Atallah and Flaherty, 2005; Shamseddine and Farhat, 2011;

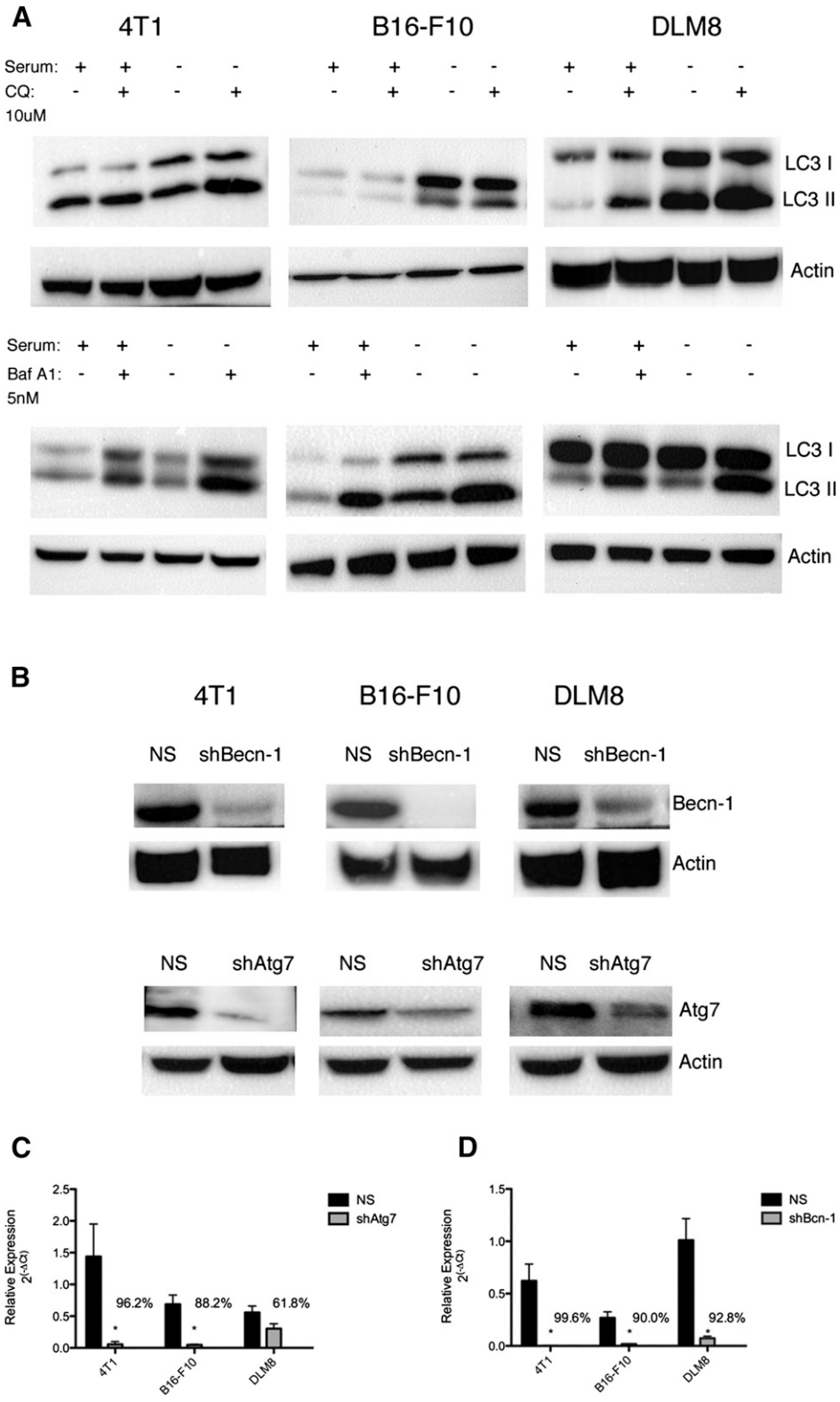

Fig. 1. Pharmacologic and genetic inhibition of autophagy. (A) 4T1, B16-F10, and DLM8 cells were treated with +/− (with or without) Earl's Balanced Salt Solution serum-free medium for 2 hours as a positive control for autophagy induction. Medium was also supplemented with +/− 10 μM CQ or 5 nM Baf A1 to block autophagy and prevent turnover of LC3 II. Both CQ and Baf A1 were able to block autophagy (increase LC3 II) in basal and starved conditions. (B) 4T1, B16-F10, and DLM8 cells were transduced with a lentivirus containing either a Becn 1, Atg7, or nonsilencing short hairpin RNA (NS). Both proteins are reduced compared with the NS control. RT-qPCR was then used to determine the level of Atg7 (C) or Becn-1 (D) mRNA expression, normalized to Hsp90 and Tbp. *Expression was significantly reduced in cells that received the short hairpin RNA targeted against Becn-1 or Atg7 compared with the nonsilencing control.

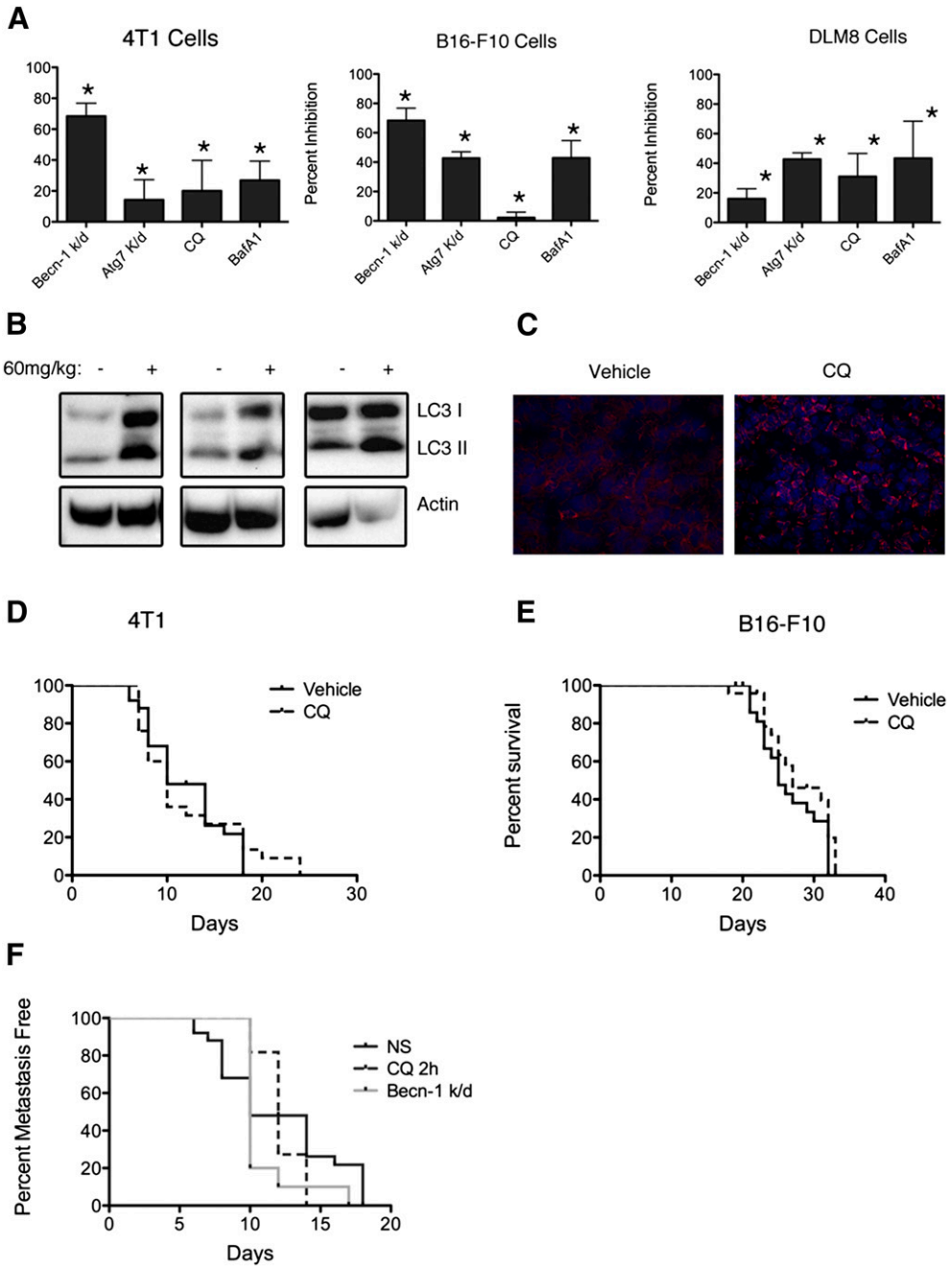

Fig. 2. Autophagy inhibition decreases cell proliferation, but not in experimentally induced metastases. (A) 4T1, B16-F10, and DLM8 cell proliferation with or without functional autophagy was assessed by Alamar Blue assay. Cells were treated for 72 hours +/− 10 μM CQ or 5 nM Baf A1. Becn 1 and Atg7 knockdown cells were grown for 72 hours. Graphs represent the mean and standard deviation of the percentage of growth inhibition compared with control cells. *Significant growth inhibition ($P < 0.05$) determined by one-sample t test using 0% as a theoretical mean. (B) Western blot analysis of liver samples from treated mice. Mice were treated daily with 60 mg/kg i.p. CQ or vehicle for 72 hours ($n = 3$). LC3 I/II increases after administration of CQ. (C) Representative images of LC3 (Cy3, red) expression in the lungs of CQ- or vehicle-treated mice. CQ-treated mice have a distinct punctate membranous and cytoplasmic pattern of immunolabeling, whereas vehicle-treated mice have a diffuse, cytosolic pattern. Kaplan-Meier event-free survival of 4T1-challenged (D) and B16-F10–challenged (E) Balb/c or C57Bl/6J mice. Mice were first pretreated with CQ and then challenged with either 4T1-luc or B16-F10 cells injected via the tail vein ($n = 25$). Mice continued to receive treatment until the development of luciferase-positive metastases or 10% weight loss. (F) Mice received 4T1-luc Becn 1 knockdown cells, cells treated with 10 μM CQ 2 hours prior, or nonsilencing (NS) control cells, and were then followed until the development of luciferase-positive metastases in the lung. k/d, knockdown.

Ruggiero et al., 2013). The combination of cisplatin, at the IC_{50} (Supplemental Fig. 2A), and autophagy inhibition had at least an additive effect on growth inhibition compared with either treatment alone, according to the Bliss independence model of synergy (Fig. 3A; Supplemental Tables 1–3). To observe the effect of autophagy inhibition in a spontaneous metastatic setting, CQ was given as either a surgical adjuvant or neoadjuvant therapy in Balb/c mice challenged with 4T1-luc cells orthotopically implanted into the mammary fat pad. Cisplatin was also given at the human equivalent exposure either in combination or as a single-agent therapy. For the surgical adjuvant model, mice received treatment 24 hours

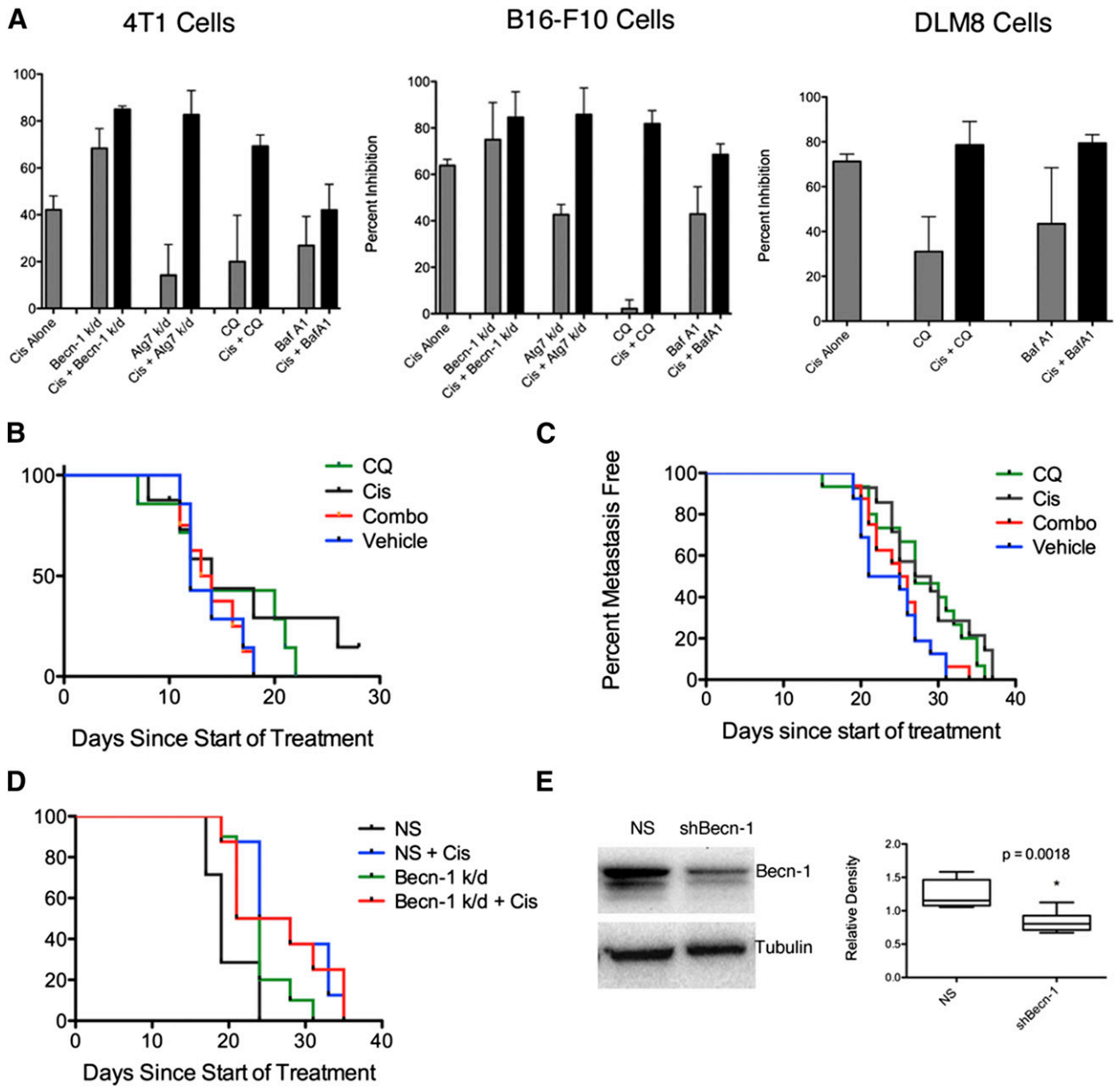

Fig. 3. CQ as a neoadjuvant therapy is able to delay metastasis, but has an antagonistic effect when given in combination with cisplatin. (A) 4T1, B16-F10, and DLM8 cell proliferation with or without functional autophagy in combination with cisplatin (Cis) was assessed by Alamar Blue assay. Cells were treated for 72 hours +/− 10 μM CQ or 5 nM Baf A1. Becn 1 and Atg7 knockdown cells were grown for 72 hours. Graphs represent the mean and standard deviation of the percentage of growth inhibition compared with control cells. (B) Time to metastatic development in lungs using adjuvant therapy. No significant difference in treatment was observed. (C) Time to metastatic development in lungs using neoadjuvant therapy. Curve represents two combined studies. There was a significant delay in metastatic development for both single-agent CQ and cisplatin since the start of treatment and after tumor removal. However, the combination therapy had an antagonistic trend. (D) Time to metastatic development in lungs using neoadjvuant cisplatin therapy in 4T1-luc-short hairpin Becn 1–challenged mice. Becn 1 knockdown, cisplatin alone, and the combination all significantly delayed metastases, but the combination did not enhance cisplatin efficacy. (E) Western blot analysis of Becn 1 expression from resected tumors. Becn 1 is still significantly decreased in the knockdown line. k/d, knockdown; NS, nonsilencing.

after resection of tumors that had reached 100 mm^3. Mice were then imaged thrice weekly until the development of luciferase-positive metastases in the lung. Metastases were not observed in any other organs. As with the experimental metastasis model, CQ had no significant effect on median time to metastatic development (Fig. 3B). However, neither did cisplatin nor the combination. Yet if mice were given neoadjuvant therapy, treatment beginning 24 hours after cell implantation, both CQ and cisplatin when administered alone were able to significantly delay metastatic development as compared with vehicle (Fig. 3C). The neoadjuvant study was repeated with similar results. Neoadjuvant treatment had no effect on primary tumor growth, and cisplatin was able to elicit more necrosis within the primary tumor compared with vehicle (Supplemental Fig. 3; Supplemental Table 4).

Interestingly, the combination was not significantly different from the vehicle, and was significantly antagonistic compared with both CQ and cisplatin (P = 0.0351 and P = 0.0399). Mice fared worse with the combination than with either CQ or cisplatin alone (CQ median time = 27 days,

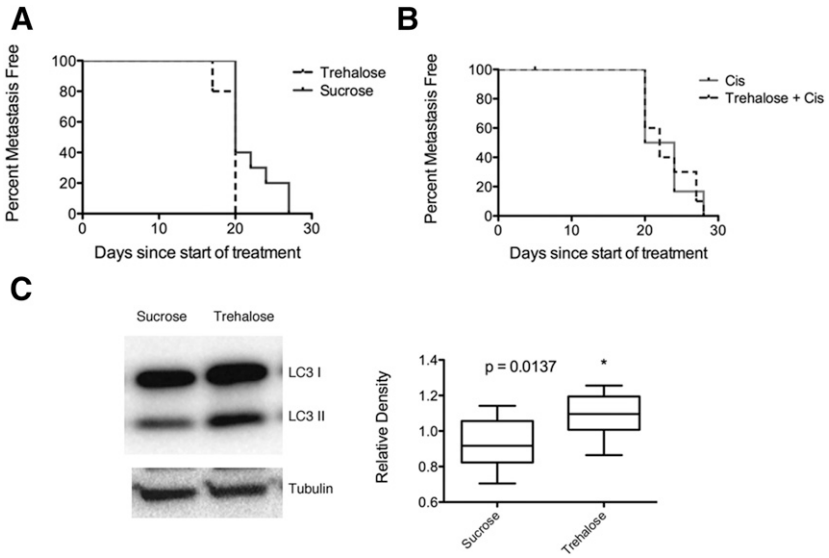

Fig. 4. Autophagy stimulation decreases the time to metastatic development. (A) 4T1-luc cells were implanted into the mammary fat pad of Balb/c mice. After a 24-hour period, mice were then given 2% trehalose or sucrose dissolved in water and received either 3 mg/kg, once every 14 days, i.p. cisplatin or vehicle. Tumors were resected at 100 mm^3. Mice were monitored thrice weekly for the development of luciferase-positive metastases in lungs. (B) Trehalose neither hindered nor enhanced cisplatin (Cis) efficacy. (C) Western blot and density analysis for LC3 processing in trehalose-treated tumors. LC3 II is significantly increased in trehalose-treated tumors.

cisplatin median time = 28.5 days, combination = 25 days). To determine if this effect was due to systemic or tumor-specific autophagy inhibition, mice were also challenged with 4T1-luc Becn 1 knockdown or nonsilencing cells and given neoadjuvant cisplatin. In this setting, autophagy inhibition by Becn 1 knockdown significantly slowed metastatic development compared with vehicle ($P = 0.0297$, median time = 22.5 vs. 19 days) (Fig. 3D). Although the Becn 1 knockdown and cisplatin combination was not as markedly antagonistic (median time = 26 vs. 24.5 days), it still did not have an additive effect, as the in vitro results suggested.

Trehalose Stimulation of Autophagy Hastens Metastatic Development. As enhanced autophagy has yet to be truly tested in a survival model, we wanted to investigate the effects of autophagy stimulation. Trehalose has been shown to be an effective inducer of autophagy, and 2% trehalose dissolved in drinking water has been used in studies investigating the protective effects of autophagy induction in neurologic and vascular disease (LaRocca et al., 2012). Similar to the other neoadjuvant models, 4T1-luc cells were orthotopically implanted, and treatment began 24 hours after either 2% sucrose or 2% trehalose with or without cisplatin dosed at the human equivalent exposure. Trehalose treatment alone shortened the time to metastatic development compared with sucrose-treated mice ($P = 0.0146$) (Fig. 4A). The addition of trehalose neither enhanced nor hindered cisplatin efficacy (Fig. 4B). LC3 I expression and LC3 II processing were significantly increased in the tumors resected from trehalose-treated mice compared with the sucrose group, indicating stimulation of autophagy (Fig. 4C).

To determine if autophagy modulation altered the metastatic characteristics of the cells, anchorage-independent growth, invasion, and migration assays were used. Trehalose did not enhance proliferation of detached cells (data not shown), nor did autophagy inhibition significantly augment growth inhibition (Fig. 5A). Neither autophagy inhibition nor stimulation altered migration or invasion significantly (Fig. 5, B and C).

Since autophagy did not appear to significantly alter the intrinsic metastatic capabilities of the cells in vitro, we explored the possibility that autophagy may influence the metastatic microenvironment to make it more growth-permissive for incoming cells. It has been demonstrated that, prior to the arrival of tumor cells, distant metastatic sites (including the lung) are primed with BMDCs coexpressing VEGFR1 and VLA-4 (integrin $\alpha_4\beta_1$), which promote vascularization, cell migration, tumor cell extravasation, and breakdown of basement membranes (Kaplan et al., 2005). Therefore, flow cytometric analysis for BMDCs was performed on the lungs and blood of mice treated with trehalose, vehicle, or CQ for 15 days, which is just prior to the development of metastases in this model (confirmed via negative luciferase imaging). There was a significant increase in cells expressing both VEGFR1 and VLA-4 in trehalose-treated mice compared with vehicle- and CQ-treated mice (lungs: $P = 0.0021$ and 0.0351, blood: $P = 0.0424$ and 0.0177) (Fig. 6). Conversely, these cells were reduced in the blood of CQ-treated mice as compared with vehicle ($P = 0.0493$). Serum was collected for multiplex cytokine analysis from trehalose- or CQ-treated mice, obtained in the same postsurgical, premetastatic window as the flow cytometric analyses of BMDCs to try and determine possible changes in cytokines that may regulate BMDC release. However, no significant differences were detected between treatment groups using a panel of 20 different cytokines, chemokines, and growth factors (data not shown). This may largely be due to the fact that our study was only able to capture a single time point. Therefore, modulating autophagy may have effects on the metastatic microenvironment that can influence cell growth, including playing a role in priming the premetastatic niche for tumor cell invasion, yet further study will be needed to elucidate the mechanism.

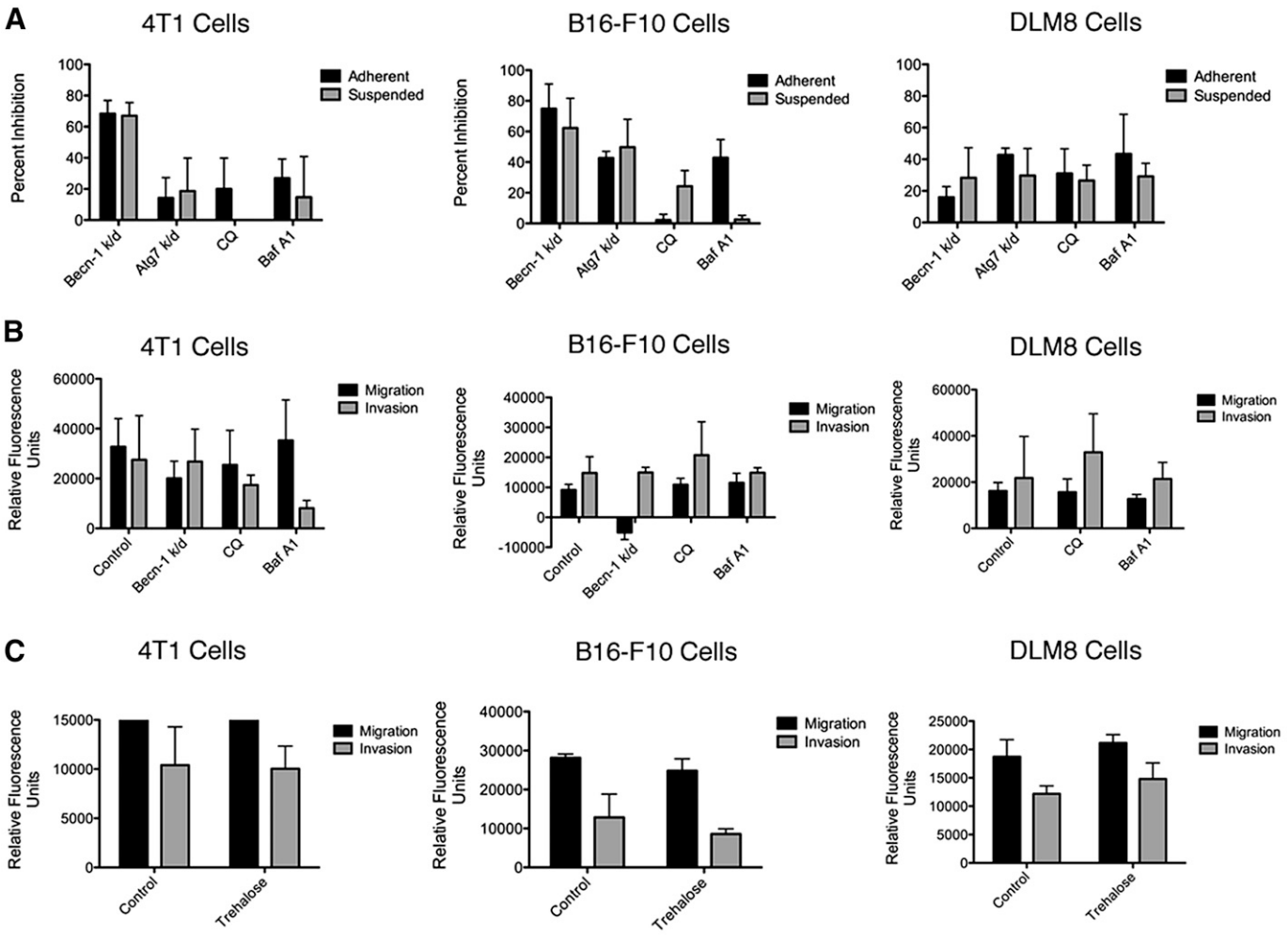

Fig. 5. Autophagy does not affect metastatic characteristics. (A) 4T1, B16-F10, and DLM8 cell proliferation with or without functional autophagy was assessed by Alamar Blue assay. Cells were treated for 72 hours +/− 10 μM CQ or 5 nM Baf A1. Becn 1 and Atg7 knockdown cells were grown for 72 hours. For anchorage-independent growth, cells were grown on poly(2-hydroxyethyl methacrylate)-coated plates to prevent attachment. Graphs represent the mean and standard deviation of the percentage of growth inhibition compared with control cells. Autophagy inhibition–induced growth inhibition was not augmented in suspended cells. (B) Autophagy inhibition did not affect the ability of 4T1, B16-F10, and DLM8 to invade or migrate. Graphs represent the mean and standard deviation of the relative fluorescence subtracted from the negative control. (C) Autophagy stimulation by 100 mM trehalose did not significantly affect migration or invasion. k/d, knockdown.

Discussion

The role of autophagy in metastasis development and progression still remains uncertain. Therefore, we sought to interrogate the effect of autophagy modulation along various stages of the metastatic cascade. Additionally, we used a variety of cancer models to address whether the effects we observed were context-dependent. As autophagy also has immunomodulatory effects, we used immune-competent mice as well as human equivalent doses rather than the maximum tolerated dose. Although CQ is the most clinically relevant and one of the most widely used autophagy inhibitors, it can affect other processes in addition to autophagy. Thus, we used another pharmacologic inhibitor, Baf A1, which is mechanistically similar to CQ, and generated several metastatic cell lines stably transfected with shRNA toward Becn 1 and Atg7.

Utilizing these various methods of autophagy inhibition in the different cancer models, we determined that autophagy inhibition alone diminished cell proliferation, although not enough to significantly alter the ability of cells to colonize the lungs in experimental 4T1 and B16-F10 metastasis models. Inhibition was tested in two settings: 1) systemic autophagy inhibition in the murine host prior to tumor challenge, and 2) autophagy impairment in cells before entry into the lungs. In both instances, autophagy inhibition was not effective at delaying metastases. These results suggest that, once the tumor cells are present in the lung, autophagy is not essential for survival. An earlier study of hepatocellular carcinoma demonstrated that autophagy was required for lung colonization due to anoikis resistance; however, the authors also noted that autophagic activity was more apparent in early-stage lesions (Peng et al., 2013).

We next tested autophagy inhibition in surgical adjuvant and neoadjuvant models. These models allow for spontaneous metastases as well as provide a more clinically relevant treatment setting. Cisplatin was also added as a treatment since it is a common therapy for all three cancer types tested here and has been shown to enhance cell death in combination with autophagy inhibition in vitro (Kaminskyy et al., 2012; Xu et al., 2012). The combination did have an additive effect on

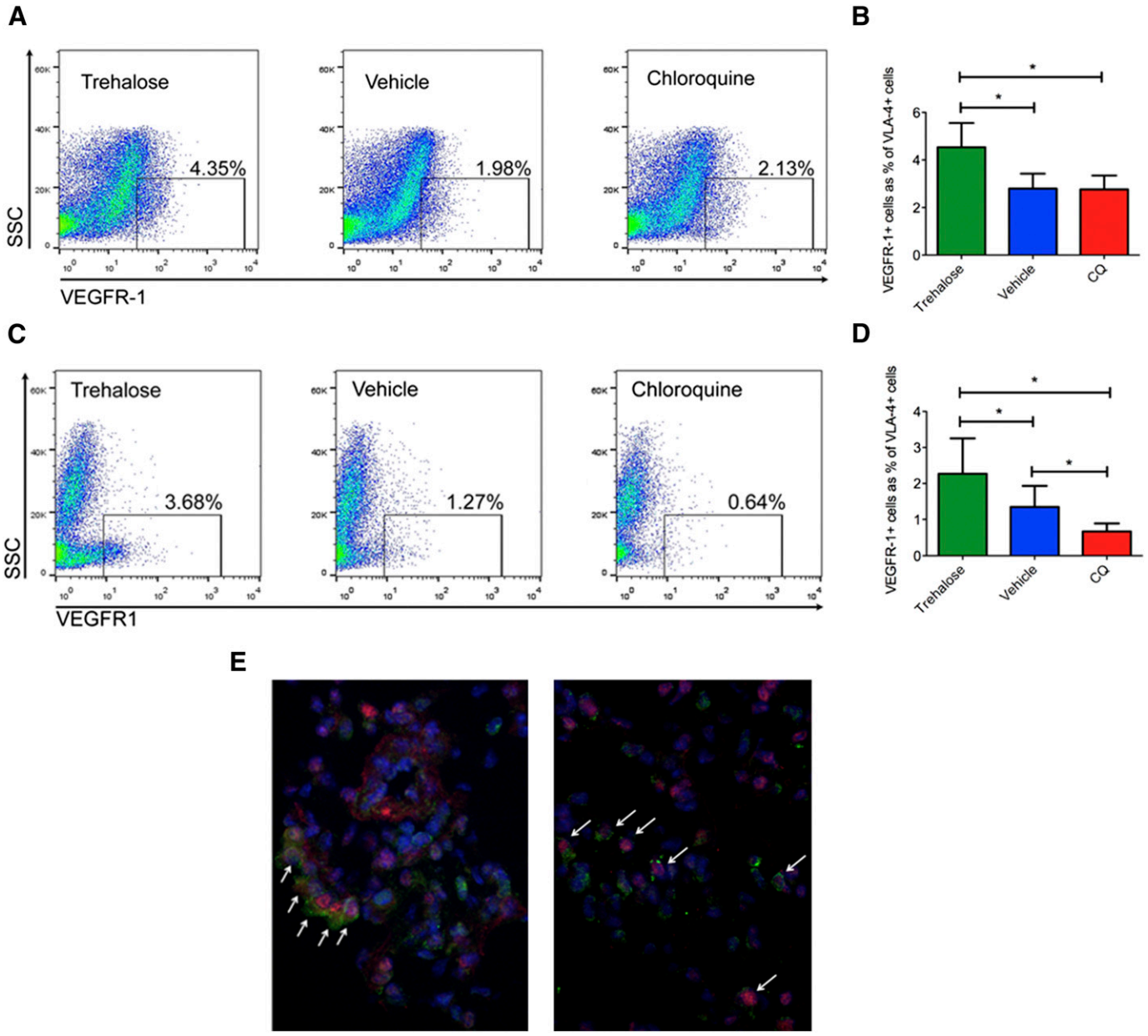

Fig. 6. Autophagy modulation corresponds to changes in BMDC number. Representative scatter plots of VEGFR1$^+$ cells in lung (A) and blood (C) with corresponding graphs (B and D). All of these cells coexpressed VLA-4, and a subset of these cells were also CD117$^+$, consistent with BMDC morphology. There are significantly more BMDCs in trehalose-treated mice. (E) Representative confocal immunofluorescent images of VEGFR1 (Cy3, red) and VLA-4 (Alexa Fluor 488, green) expression in the lungs of mice treated with trehalose before the arrival of tumor cells. White arrows indicate double positive cells, indicative of BMDCs.

inhibiting cell growth in vitro, but similar to the i.v.-delivered metastases, there was no delay in metastatic development by any treatment in the surgical adjuvant model. Yet, in the neoadjuvant model, CQ alone was able to slow time to progression. This was recapitulated using the Becn 1 knockdown line, suggesting that these effects are due to a tumor cell autonomous effect of autophagy. The fact that autophagy inhibition only has an effect in the neoadjuvant model and not the other models suggests that the importance of autophagy lies in the very early events of the metastatic cascade. Although more potent inhibitors of autophagy could show more efficacy than CQ as adjuvant therapy, the response will still likely be better before cells have had a chance to reach the metastatic site (McAfee et al., 2012). Future studies should also examine autophagy inhibition for cancers that metastasize to other sites, such as bone, to see if these results are specific to metastasis to the lung.

The combination of cisplatin and CQ actually had a significantly antagonistic effect, although it was not as pronounced with genetically inhibited autophagy. This could indicate that the systemic loss of autophagy alters the surrounding environment, or the knockdowns were only partially effective. Autophagy has been shown to have many immune-related effects, including antigen presentation, differentiation, and recruitment of dendritic cells to participate in immunogenic cell death. A similar effect was observed by Ko et al. (2014) with the combination of autophagy inhibition and radiation. In culture and in nude mice, autophagy inhibition sensitized to radiation,

but in the immune-competent Balb/c model, the combination was ineffective. Additionally, autophagy appears to be required for the release of ATP from dying tumor cells (Michaud et al., 2011). This extracellular ATP facilitates the recruitment of immature myeloid cells and can promote their differentiation into dendritic cells capable of capturing tumor-derived antigens and priming cytotoxic immune cells, such as CD8+ T cells. Therefore, one possible explanation for the observed antagonism between cisplatin and CQ could be due to autophagy's role in immune-cell recruitment. Further study assessing immune-cell populations at different time points during metastatic development will be needed to resolve the relationship between cisplatin and immune-driven cytotoxicity. By inhibiting autophagy, there may be unanticipated and even counterproductive results related to alterations within the metastatic microenvironment.

Since a survival model examining the effects of autophagy stimulation has not been tested to date, we used the disaccharide trehalose to induce autophagy in our neoadjuvant model. Although systemic autophagy inhibition appeared to abrogate cisplatin efficacy, autophagy stimulation neither hindered nor enhanced cisplatin efficacy. Where autophagy inhibition was able to slow metastasis, trehalose-induced autophagy correspondingly accelerated metastasis development. Since autophagy only seemed to influence metastatic growth early, before cells have escaped the primary tumor, we examined the effect of autophagy modulation on the metastatic characteristics necessary to precipitate this event. There was no difference in growth inhibition overall, whether cells were allowed to adhere or were suspended. If autophagy inhibition was critical to anchorage-independent growth, there should have been augmented growth inhibition in the suspended cells compared with the adherent ones. Trehalose was also unable to enhance anchorage-independent growth or adherent cell proliferation. Similarly, there was still no change in the ability of cells to invade and migrate when autophagy was altered. Other studies have also indicated that autophagy inhibition may not necessarily alter migration or invasion, but does impact anchorage-independent growth (Fung et al., 2008; Macintosh et al., 2012; Peng et al., 2013). The development of anoikis resistance is likely not universally dependent on autophagy, and some cancer types may be more likely to use autophagy to develop anchorage-independent growth.

As autophagy did not affect the intrinsic metastatic capabilities of the cells, we wanted to explore the potential for autophagy to modulate the metastatic microenvironment as a possible mechanism for the observed differences in metastatic growth between treatments. We chose to measure BMDCs, particularly those expressing vascular endothelial growth factor receptor 1 (VEGFR1)/Integrin $\alpha4\beta1$ very late antigen-4 (VLA-4), as these cells have been shown to infiltrate the lung, change the microenvironment, and generate a permissive niche for the subsequent arrival of tumor cells. These cells activate other integrins and chemokines, such as stromal cell-derived factor 1 (CXCL12), that not only recruit CXC receptors-4–expressing tumor cells to the site of metastasis, but also promote their attachment, survival, and vascularization (Peinado et al., 2011). These cells are mobilized to the lung or other metastatic sites by chemokines secreted by the primary tumor cells and stroma to prepare the way for the incoming tumor cells (Peinado et al., 2011). The number of cells expressing VEGFR1/VLA-4 was measured in the lungs and blood of mice after autophagy modulation but before the arrival of tumor cells. There was a significant increase in $VEGFR1^+\backslash VLA\text{-}4^+$ cells in the trehalose-treated mice and further reduction in the CQ-treated mice, notably within circulation. Autophagy may be cytoprotective in bone marrow–derived stem cells, including endothelial progenitor cells (Herberg et al., 2013; Wang et al., 2013). Additionally, autophagy can regulate cytokine secretion in RAS-transformed and breast cancer models (Lock et al., 2014; Maycotte et al., 2015). Therefore, the increased levels of autophagy in the trehalose-treated mice may provide an advantage toward the survival and/or recruitment of bone marrow–derived $VEGFR1^+$ cells and allow for the formation of a more growth-permissive metastatic microenvironment. Thus, autophagy modulation also likely influences the secretion of tumor-derived soluble factors. Autophagy-mediated alterations in these systemic cytokine levels could have a significant impact on both the tumor-mediated priming of the lung microenvironment necessary for adhesion and retention of BMDCs, as well as the subsequent ability of BMDCs within the premetastatic niche to secrete the chemokines required for mobilization of metastasizing tumor cells. To address this, we collected serum for multiplex cytokine analysis from trehalose- or CQ-treated mice, obtained in the same postsurgical, premetastatic window as the flow cytometric analyses of BMDCs within the lung and blood. However, we did not detect any significant differences between treatment groups using a panel of 20 different cytokines, chemokines, and growth factors (data not shown). Our study was limited in that we only captured a single time point for cytokine analysis, and future studies designed to more thoroughly investigate the kinetics of cytokine secretion during primary tumor growth and metastasis development would be necessary to determine if the ability of autophagy to regulate cytokine release could influence BMDC recruitment and niche formation. Additional studies combining genetic models of autophagy inhibition and stimulation will also be needed to determine if these effects are specific to autophagy.

Conclusions

Although autophagy has been identified as a potential mechanism of survival and resistance for tumor cells, it is still unclear exactly how cells use autophagy while undergoing metastatic dissemination. Understanding this role can allow us to maximize the potential of autophagy inhibition as a therapy. In this study, we observed that modulating autophagy only affected metastatic development if administered in the early stages of metastatic disease, prior to the arrival of tumor cells in the lung. We present the possibility that the efficacy of autophagy inhibition may be microenvironment-related, particularly in the developing premetastatic niche. However, once cells have been established, functional autophagy of the microenvironment may actually keep cell growth in check, as it could alter the phenotype or recruitment of immune-cell populations. Consequently, caution is recommended in combining therapies, particularly if cytotoxicity can be attributed to immune-related cell death. Pharmacologic autophagy inhibition may have effects outside of the tumor, including changes in the surrounding microenvironment that may not be detectable in immune-deficient models. Continued studies will be best served by using multiple avenues of data

collection, including cell culture, xenografts, and immune-competent model organisms, to develop a more complete picture of autophagy inhibition in the context of an anticancer therapy.

Authorship Contributions

Participated in research design: Barnard, Regan, Hansen, Thorburn, Gustafson.

Conducted experiments: Barnard, Regan, Hansen.

Contributed new reagents or analytic tools: Maycotte.

Performed data analysis: Barnard, Regan, Hansen.

Wrote or contributed to the writing of the manuscript: Barnard, Regan, Hansen, Maycotte, Thorburn, Gustafson.

References

Amaravadi RK, Lippincott-Schwartz J, Yin XM, Weiss WA, Takebe N, Timmer W, DiPaola RS, Lotze MT, and White E (2011) Principles and current strategies for targeting autophagy for cancer treatment. *Clin Cancer Res* **17**:654–666.

Asai T, Ueda T, Itoh K, Yoshioka K, Aoki Y, Mori S, and Yoshikawa H (1998) Establishment and characterization of a murine osteosarcoma cell line (LM8) with high metastatic potential to the lung. *Int J Cancer* **76**:418–422.

Aslakson CJ and Miller FR (1992) Selective events in the metastatic process defined by analysis of the sequential dissemination of subpopulations of a mouse mammary tumor. *Cancer Res* **52**:1399–1405.

Atallah E and Flaherty L (2005) Treatment of metastatic malignant melanoma. *Curr Treat Options Oncol* **6**:185–193.

Avivar-Valderas A, Salas E, Bobrovnikova-Marjon E, Diehl JA, Nagi C, Debnath J, and Aguirre-Ghiso JA (2011) PERK integrates autophagy and oxidative stress responses to promote survival during extracellular matrix detachment. *Mol Cell Biol* **31**:3616–3629.

Barnard RA, Wittenburg LA, Amaravadi RK, Gustafson DL, Thorburn A, and Thamm DH (2014) Phase I clinical trial and pharmacodynamic evaluation of combination hydroxychloroquine and doxorubicin treatment in pet dogs treated for spontaneously occurring lymphoma. *Autophagy* **10**:1415–1425.

Bristol ML, Emery SM, Maycotte P, Thorburn A, Chakradeo S, and Gewirtz DA (2013) Autophagy inhibition for chemosensitization and radiosensitization in cancer: do the preclinical data support this therapeutic strategy? *J Pharmacol Exp Ther* **344**:544–552.

Caino MC, Chae YC, Vaira V, Ferrero S, Nosotti M, Martin NM, Weeraratna A, O'Connell M, Jernigan D, and Fatatis A, et al. (2013) Metabolic stress regulates cytoskeletal dynamics and metastasis of cancer cells. *J Clin Invest* **123**:2907–2920.

Casper ES, Kelsen DP, Alcock NW, and Lewis JL, Jr (1983) Ip cisplatin in patients with malignant ascites: pharmacokinetic evaluation and comparison with the iv route. *Cancer Treat Rep* **67**:235–238.

Degenhardt K, Mathew R, Beaudoin B, Bray K, Anderson D, Chen G, Mukherjee C, Shi Y, Gélinas C, and Fan Y, et al. (2006) Autophagy promotes tumor cell survival and restricts necrosis, inflammation, and tumorigenesis. *Cancer Cell* **10**:51–64.

DeNardo DG, Barreto JB, Andreu P, Vasquez L, Tawfik D, Kolhatkar N, and Coussens LM (2009) CD4(+) T cells regulate pulmonary metastasis of mammary carcinomas by enhancing protumor properties of macrophages. *Cancer Cell* **16**:91–102.

Fidler IJ (1975) Biological behavior of malignant melanoma cells correlated to their survival in vivo. *Cancer Res* **35**:218–224.

Fung C, Lock R, Gao S, Salas E, and Debnath J (2008) Induction of autophagy during extracellular matrix detachment promotes cell survival. *Mol Biol Cell* **19**:797–806.

Gewirtz DA (2014) When cytoprotective autophagy isn't… and even when it is. *Autophagy* **10**:391–392.

Herberg S, Shi X, Johnson MH, Hamrick MW, Isales CM, and Hill WD (2013) Stromal cell-derived factor-1β mediates cell survival through enhancing autophagy in bone marrow-derived mesenchymal stem cells. *PLoS One* **8**:e58207.

Ichimura Y and Komatsu M (2011) Pathophysiological role of autophagy: lesson from autophagy-deficient mouse models. *Exp Anim* **60**:329–345.

Kaminskyy VO, Piskunova T, Zborovskaya IB, Tchevkina EM, and Zhivotovsky B (2012) Suppression of basal autophagy reduces lung cancer cell proliferation and enhances caspase-dependent and -independent apoptosis by stimulating ROS formation. *Autophagy* **8**:1032–1044.

Kaplan RN, Riba RD, Zacharoulis S, Bramley AH, Vincent L, Costa C, MacDonald DD, Jin DK, Shido K, and Kerns SA, et al. (2005) VEGFR1-positive haematopoietic bone marrow progenitors initiate the pre-metastatic niche. *Nature* **438**:820–827.

Kenific CM, Thorburn A, and Debnath J (2010) Autophagy and metastasis: another double-edged sword. *Curr Opin Cell Biol* **22**:241–245.

Ko A, Kanehisa A, Martins I, Senovilla L, Chargari C, Dugue D, Mariño G, Kepp O, Michaud M, and Perfettini JL, et al. (2014) Autophagy inhibition radiosensitizes in vitro, yet reduces radioresponses in vivo due to deficient immunogenic signalling. *Cell Death Differ* **21**:92–99.

Kubota T, Inoue S, Furukawa T, Ishibiki K, Kitajima M, Kawamura E, and Hoffman RM (1993) Similarity of serum-tumor pharmacokinetics of antitumor agents in man and nude mice. *Anticancer Res* **13** (5A):1481–1484.

LaRocca TJ, Henson GD, Thorburn A, Sindler AL, Pierce GL, and Seals DR (2012) Translational evidence that impaired autophagy contributes to arterial ageing. *J Physiol* **590**:3305–3316.

Lazova R, Camp RL, Klump V, Siddiqui SF, Amaravadi RK, and Pawelek JM (2012) Punctate LC3B expression is a common feature of solid tumors and associated with proliferation, metastasis, and poor outcome. *Clin Cancer Res* **18**:370–379.

Lock R, Kenific CM, Leidal AM, Salas E, and Debnath J (2014) Autophagy-dependent production of secreted factors facilitates oncogenic RAS-driven invasion. *Cancer Discov* **4**:466–479.

Lopez-Flores A, Jurado R, and Garcia-Lopez P (2005) A high-performance liquid chromatographic assay for determination of cisplatin in plasma, cancer cell, and tumor samples. *J Pharmacol Toxicol Methods* **52**:366–372.

Macintosh RL, Timpson P, Thorburn J, Anderson KI, Thorburn A, and Ryan KM (2012) Inhibition of autophagy impairs tumor cell invasion in an organotypic model. *Cell Cycle* **11**:2022–2029.

Mahalingam D, Mita M, Sarantopoulos J, Wood L, Amaravadi RK, Davis LE, Mita AC, Curiel TJ, Espitia CM, and Nawrocki ST, et al. (2014) Combined autophagy and HDAC inhibition: a phase I safety, tolerability, pharmacokinetic, and pharmacodynamic analysis of hydroxychloroquine in combination with the HDAC inhibitor vorinostat in patients with advanced solid tumors. *Autophagy* **10**:1403–1414.

Maycotte P, Aryal S, Cummings CT, Thorburn J, Morgan MJ, and Thorburn A (2012) Chloroquine sensitizes breast cancer cells to chemotherapy independent of autophagy. *Autophagy* **8**:200–212.

Maycotte P, Gearheart CM, Barnard R, Aryal S, Mulcahy Levy JM, Fosmire SP, Hansen RJ, Morgan MJ, Porter CC, and Gustafson DL, et al. (2014) STAT3-mediated autophagy dependence identifies subtypes of breast cancer where autophagy inhibition can be efficacious. *Cancer Res* **74**:2579–2590.

Maycotte P, Jones KL, Goodall ML, Thorburn J, and Thorburn A (2015) Autophagy Supports Breast Cancer Stem Cell Maintenance by Regulating IL6 Secretion. *Mol Cancer Res* **13**:651–658.

McAfee Q, Zhang Z, Samanta A, Levi SM, Ma XH, Piao S, Lynch JP, Uehara T, Sepulveda AR, and Davis LE, et al. (2012) Autophagy inhibitor Lys05 has single-agent antitumor activity and reproduces the phenotype of a genetic autophagy deficiency. *Proc Natl Acad Sci USA* **109**:8253–8258.

Michaud M, Martins I, Sukkurwala AQ, Adjemian S, Ma Y, Pellegatti P, Shen S, Kepp O, Scoazec M, and Mignot G, et al. (2011) Autophagy-dependent anticancer immune responses induced by chemotherapeutic agents in mice. *Science* **334**:1573–1577.

Mizushima N and Yoshimori T (2007) How to interpret LC3 immunoblotting. *Autophagy* **3**:542–545.

Mizushima N, Yoshimori T, and Levine B (2010) Methods in mammalian autophagy research. *Cell* **140**:313–326.

Ni HM, Bockus A, Wozniak AL, Jones K, Weinman S, Yin XM, and Ding WX (2011) Dissecting the dynamic turnover of GFP-LC3 in the autolysosome. *Autophagy* **7**:188–204.

Peinado H, Lavotshkin S, and Lyden D (2011) The secreted factors responsible for pre-metastatic niche formation: old sayings and new thoughts. *Semin Cancer Biol* **21**:139–146.

Peng YF, Shi YH, Ding ZB, Ke AW, Gu CY, Hui B, Zhou J, Qiu SJ, Dai Z, and Fan J (2013) Autophagy inhibition suppresses pulmonary metastasis of HCC in mice via impairing anoikis resistance and colonization of HCC cells. *Autophagy* **9**:2056–2068.

Pfaffl MW (2001) A new mathematical model for relative quantification in real-time RT-PCR. *Nucleic Acids Res* **29**:e45.

Rangwala R, Chang YC, Hu J, Algazy KM, Evans TL, Fecher LA, Schuchter LM, Torigian DA, Panosian JT, and Troxel AB, et al. (2014a) Combined MTOR and autophagy inhibition: phase I trial of hydroxychloroquine and temsirolimus in patients with advanced solid tumors and melanoma. *Autophagy* **10**:1391–1402.

Rangwala R, Leone R, Chang YC, Fecher LA, Schuchter LM, Kramer A, Tan KS, Heitjan DF, Rodgers G, and Gallagher M, et al. (2014b) Phase I trial of hydroxychloroquine with dose-intense temozolomide in patients with advanced solid tumors and melanoma. *Autophagy* **10**:1369–1379.

Reece PA, Stafford I, Russell J, Khan M, and Gill PG (1987) A model for ultrafilterable plasma platinum disposition in patients treated with cisplatin. *Cancer Chemother Pharmacol* **20**:26–32.

Rosenfeld MR, Ye X, Supko JG, Desideri S, Grossman SA, Brem S, Mikkelson T, Wang D, Chang YC, and Hu J, et al. (2014) A phase I/II trial of hydroxychloroquine in conjunction with radiation therapy and concurrent and adjuvant temozolomide in patients with newly diagnosed glioblastoma multiforme. *Autophagy* **10**:1359–1368.

Ruggiero A, Trombatore G, Triarico S, Arena R, Ferrara P, Scalzone M, Pierri F, and Riccardi R (2013) Platinum compounds in children with cancer: toxicity and clinical management. *Anticancer Drugs* **24**:1007–1019.

Shamseddine AI and Farhat FS (2011) Platinum-based compounds for the treatment of metastatic breast cancer. *Chemotherapy* **57**:468–487.

Taetle R, Rosen F, Abramson I, Venditti J, and Howell S (1987) Use of nude mouse xenografts as preclinical drug screens: in vivo activity of established chemotherapeutic agents against melanoma and ovarian carcinoma xenografts. *Cancer Treat Rep* **71**:297–304.

Tuloup-Minguez V, Hamaï A, Greffard A, Nicolas V, Codogno P, and Botti J (2013) Autophagy modulates cell migration and β1 integrin membrane recycling. *Cell Cycle* **12**:3317–3328.

van Hennik MB, van der Vijgh WJ, Klein I, Elferink F, Vermorken JB, Winograd B, and Pinedo HM (1987) Comparative pharmacokinetics of cisplatin and three analogues in mice and humans. *Cancer Res* **47**:6297–6301.

Vogl DT, Stadtmauer EA, Tan KS, Heitjan DF, Davis LE, Pontiggia L, Rangwala R, Piao S, Chang YC, and Scott EC, et al. (2014) Combined autophagy and proteasome inhibition: a phase 1 trial of hydroxychloroquine and bortezomib in patients with relapsed/refractory myeloma. *Autophagy* **10**:1380–1390.

Wang HJ, Zhang D, Tan YZ, and Li T (2013) Autophagy in endothelial progenitor cells is cytoprotective in hypoxic conditions. *Am J Physiol Cell Physiol* **304**:C617–C626.

Xu Y, Yu H, Qin H, Kang J, Yu C, Zhong J, Su J, Li H, and Sun L (2012) Inhibition of autophagy enhances cisplatin cytotoxicity through endoplasmic reticulum stress in human cervical cancer cells. *Cancer Lett* **314**:232–243.

Yoshimori T, Yamamoto A, Moriyama Y, Futai M, and Tashiro Y (1991) Bafilomycin A1, a specific inhibitor of vacuolar-type H(+)-ATPase, inhibits acidification and protein degradation in lysosomes of cultured cells. *J Biol Chem* **266**:17707–17712.

Address correspondence to: Daniel L. Gustafson, Flint Animal Cancer Center, Colorado State University, Department of Clinical Sciences, 300 West Drake Street, Fort Collins, CO 80523. E-mail: Daniel.Gustafson@colostate.edu